International Journal of Pharmaceutics 643 (2023) 123230

Contents lists available at ScienceDirect

International Journal of Pharmaceutics

journal homepage: www.elsevier.com/locate/ijpharm

Novel liposomal formulations for protection and delivery of levodopa: Structure-properties correlation

Elena Allegritti [a], Sara Battista [a,1], Maria Anna Maggi [b], Claudia Marconi [c], Luciano Galantini [c], Luisa Giansanti [a,*]

[a] Dipartimento di Scienze Fisiche e Chimiche, Università degli Studi dell'Aquila, Via Vetoio, 67010 Coppito, AQ, Italy
[b] Hortus Novus, Via Campo Sportivo 2, Canistro, 67051 L'Aquila, Italy
[c] Dipartimento di Chimica, Università di Roma "Sapienza", Piazzale Aldo Moro 5, 00185 Roma, Italy

ARTICLE INFO

Keywords:
Parkinson's disease
Levodopa
Intranasal delivery
Liposomes
Antiradical activity
N-oxide moiety

ABSTRACT

Liposomes are promising drug carriers for a wide range of central nervous system disorders, such as Parkinson's disease (PD), since they can protect active substances from degradation and could be administered intranasally, ensuring a direct access to the brain. Levodopa (LD), the drug commonly used to treat PD, spontaneously oxidizes in aqueous solutions and thus needs to be stabilized. Our investigation focuses on the preparation and the physico-chemical characterization of mixed liposomes to vehiculate LD and two natural substances (*L*-ascorbic acid and quercetin) that can prevent its oxidation and contribute to the treatment of Parkinson's disease. These co-loaded vesicles were prepared using a saturated phospholipid and structurally related cationic or analogue *N*-oxide surfactants and showed different properties, based on their composition. In particular, *ex-vivo* permeability tests using porcine nasal mucosa were performed, denoting that subtle variations of the lipids structure can significantly affect the delivery of LD to the target site.

1. Introduction

Parkinson's disease (PD) is the second most common neurodegenerative disorder, and it affects 1% of the world population aged 60 years and above. This condition, to which oxidative stress also contributes (Jenner, 2003), is characterized by the death of dopaminergic neurons in the substantia nigra, resulting in low dopamine concentration in the encephalon and movement disorders in patients (Darden, 2007). Dopamine cannot penetrate the blood–brain barrier (BBB) and reach the brain, so it has no therapeutic effect in parkinsonism. There is no cure for PD, anyway treatments based on levodopa (LD, Chart 1**A**) can help to reduce the symptoms and improve patient's quality of life. LD is a precursor in the pathway of dopamine synthesis, is carried across the barrier by an *L*-amino acid transporter and can get to the target site, where it is decarboxylated by an enzyme to dopamine (Lewitt, 2008). LD, orally administered, is absorbed from the intestine but only an amount less than 3% enters the brain unaffected so, as a consequence, it must be given in large quantities to reach the minimum therapeutic concentration, leading to significant side effects (Ferreira et al., 2015). Moreover, it is light sensitive and easily oxidized to melanins in aqueous medium becoming inactive (Fitzpatrick, 1950). Despite these limitations, LD remains the gold standard in the treatment of PD.

Among all the noninvasive methods for the administration of a drug, the intranasal ruote grants a direct access to the brain, avoiding the need to cross the BBB (Emad et al., 2021); that is particularly important in the case of bioactive compounds that work on the central nervous system, such as antiparkinson agents. The effectiveness of intranasal therapy depends on the ability of the drug to penetrate the nasal mucosa and to its physical and chemical properties: the molecular weight, the charge, the polarity and, of course, the resistance to hydrolytic and redox enzyme that are present on the mucosa (Costantino et al., 2007). A limiting factor is the mucociliary clearance, which is a defense mechanism of the respiratory system: when xenobiotics interact with the nasal mucosa, they are rapidly eliminated through the digestive system. In the past few years, liposomes have gained a lot of attention as drug carriers because of their biocompatibility and their ability to entrap both polar and non-polar molecules, protecting them from the surrounding environment. Besides, it was demonstrated by several researches that they

* Corresponding author.
E-mail address: luisa.giansanti@univaq.it (L. Giansanti).
[1] Sara Battista: Institut de Ciéncia de Materials de Barcelona (ICMAB - CSIC) Campus U.A.B., 08193 Bellaterra, Barcelona (Spain).

https://doi.org/10.1016/j.ijpharm.2023.123230
Received 21 April 2023; Received in revised form 11 July 2023; Accepted 13 July 2023
Available online 16 July 2023

show mucoadhesive properties, making them good candidates for intranasal delivery. Zheng and coworkers demonstrated the higher effectiveness of nasal delivery of a hydrophilic β-amyloid protein breaker peptide loaded in liposomes with respect to the free drug administered intravenously in terms of residence time and brain uptake (Zheng et al., 2015); liposomal intranasal delivery of ferric ammonium citrate for the treatment of iron deficiency anemia increased the level of drug with respect to intranasal administration of a solution of the free drug in all brain sections one day after the last treatment, in particular in the olfactory bulb one, through which the drug enters into the brain (Guo et al., 2017). Also liposomal lipophilic drugs can be delivered to the brain after intranasal administration. The use of liposomes allows to overcome the problems due to low solubility of the molecules, brings to a longer duration of therapeutic effects, high concentration and prolonged drug distribution into the brain (Hong et al., 2019). The brain and systemic bioavailability of donepezil increased when it was included in liposomes and intranasally administered. Moreover, it was demonstrated that drug transport to the brain occurs either via direct and indirect pathways (Al Asmari et al., 2016).

Another advantage linked to the use of liposomes as drug delivery systems is that it is possible to modify their surface by functionalization with polyethylene glycol to prolong their circulation time by reducing the absorption of opsonins (Abbina and Parambath, 2018; Mohamed et al., 2019) or other molecules such as aptamers, antibodies or peptides and so increase their specificity towards the target tissue (Riaz et al., 2018). In particular, liposomes functionalized with chlorotoxin, a 36-amino acid natural peptide extracted from a scorpion venom, including LD were prepared to deliver it to the brain. This formulation showed an increased uptake by brain microvascular endothelial cells, an increased accumulation of LD metabolites in the brain and a reduction in behavioral disorders in mice (Xiang et al., 2012). Anyway, the used peptide is very expensive and this aspect limits the potential commercialization of this formulation. Moreover, the investigated formulation lacks a proper antioxidant inside liposomes to prevent LD oxidation. Liposomes functionalized with maltodextrins and glutathione as antioxidant showed a good LD entrapment efficiency and an increased permeability to the BBB with respect to free LD, but the formulations showed tendency to aggregate yet after one week (Gurturk et al., 2017). Cationic liposomal LD forms containing *L*-ascorbic acid (AA), curcumin or superoxide dismutase as antioxidant were also investigated (García Esteban et al., 2018): they showed good entrapment efficiency and stability, but a relatively fast release of the entrapped LD (3 h) and high dimensions (diameter higher than 1 μm, reduced to 600 nm after extrusion); this limitation hampers their use as LD delivery systems because it is known that liposomes featuring diameters higher than 200 nm are rapidly cleared by macrophages in the reticuloendothelial system with a consequent high clearance (Brandl, 2001).

The physicochemical properties of liposomes strongly depend on the chemical structure of the monomers by which there are formed: alkyl chain length, the presence or the absence of one or more unsaturations, varying the hydrophilic/hydrophobic balance of the molecules, can significantly affect the fluidity of the bilayer and the interaction with solutes included in the vesicles (Battista et al., 2020c; Bordi et al., 2010; Mohammadi et al., 2016). Also pH-sensitivity (Liskayová et al., 2019; Giansanti et al., 2019; Abri Aghdam et al., 2019; Karanth and Murthy, 2010) and chirality (Bombelli et al., 2010, 2008; Ishigami et al., 2015; Wang et al., 2023) can play a crucial role in lipid organization, in the release of loaded drug and in liposomes internalization and uptake; the charge of the polar headgroup (Battista et al., 2020c; Bombelli et al., 2010, 2008; Bordi et al., 2010; Gabizon and Papahadjopoulos, 1992; Giansanti et al., 2016; Kleszczyńska et al., 2000) and/or the nature of counterions (Feitosa et al., 2023; Oliveira et al., 2016; Shang et al., 2001) influence the ability of the aggregates to interact with target cells, membrane permeability and the entrapment efficiency of the loaded active principles. The inclusion of surfactants can destabilize the vesicle bilayers allowing the change of shape and volume at minimal energetic cost: in this way, liposomes become more elastic (Bnyan et al., 2018; Marwah et al., 2020). Furthermore, the addition of surfactants into liposomal bilayer can modify the physical and chemical properties of the vesicles (Resende et al., 2023; Tai et al., 2017). Among all the different classes of amphiphilic molecules, we were attracted by *N*-oxide and quaternary ammonium ones. *N*-oxide (*N*-ox) surfactants are biodegradable and non-toxic (Singh et al., 2006); their charge depends on the pH of the medium, but they are non-ionic under physiological condition. They were already used to prepare pH-sensitive liposomes (Liskayová et al., 2019). In addition, they turned out to be interesting since they exhibit antioxidant (Piasecki et al., 2008), antiperoxidative (Krasowska et al., 2007) and antiradical properties (Lewińska et al., 2021). Quaternary ammonium surfactants, as well, proved to possess antioxidant activity, being able to reduce the oxidation of the membrane lipids of pig erythrocytes (Kleszczyńska et al., 2000).

Based on this premises, we prepared mixed liposomes for the delivery of LD composed of a saturated natural phospholipid (1,2-dimyristoyl-*sn*-glycero-3-phosphocholine, DMPC) and one of the micelle-forming surfactants reported in Chart 1**B** in two different molar ratios, 9:1 and 7:3. All the surfactants possess the same chain length, but they differ for the polar headgroup: two of them bear the *N*-ox moiety, while the other two own the quaternary ammonium group. Thanks to the presence of the pyrrolidinium ring, the *L*-prolinol derivatives possess a lower degree of freedom if compared to their acyclic analogues; this feature influences the volume and the hydration of the headgroup (Karukstis and McDonough, 2005). C**14** and C**14** *N*-ox, were synthesized and characterized (critical micellar concentration and pK_a values) in a previous work (Battista et al., 2019): they showed the ability *i*) to increase the antiradical activity of substrates included in micelles they form and *ii*) to improve the efficacy as delivery systems of the liposomes in which they are included. The systematic structural variation of the four surfactants used in this investigation for the formulation of mixed

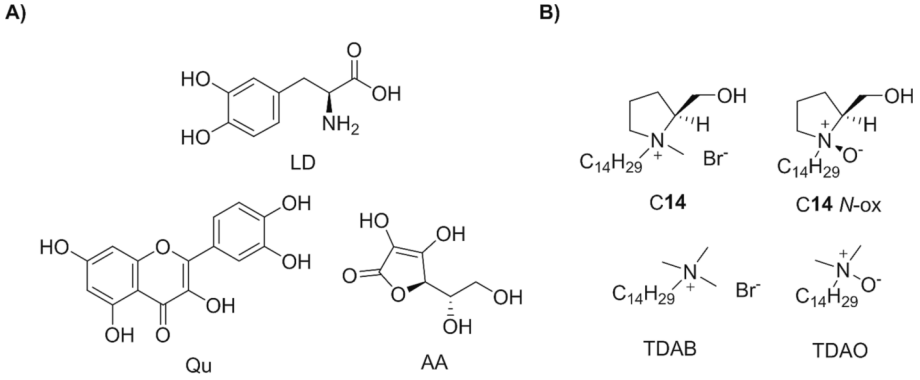

Chart 1. Structure of the molecules vehiculated (**A**) and of the surfactants used in liposomal formulations (**B**).

liposomes allowed us to investigate in detail either the role of the charge and of the rigidity of the polar region and the eventual synergy of these structural features.

Two powerful natural antioxidants, the hydrophilic AA (Chart 1**A**) and the hydrophobic quercetin (Qu, Chart 1**A**), were added to the formulations in order to prevent prodrug oxidation and to retard the progression of PD (Filograna et al., 2016; Jin et al., 2014). Infact, AA can protect neuronal cells against damages induced by reactive oxygen species and reduce the consumption of endogenous scavenging antioxidants (Varshosaz et al., 2014). AA, being polar, was loaded into the aqueous core of liposomes together with LD by passive loading and directly inhibited its oxidation to melanins. On the contrary, Qu was disposed in the lipid bilayer reacting with the oxygen that eventually crosses the membrane and thus obstructing it from reaching the prodrug. Literature reports that the best LD/AA ratio to prevent LD oxidation is 5:1, so we choose this ratio in this investigation (García Esteban et al., 2018). We previously demonstrated that C**14** and C**14** *N*-ox or their analogues (Battista et al., 2022a, 2020a; Bombelli et al., 2008) can in most cases increase the antiradical activity and the efficacy of the molecules vehiculated in the aggregates they form (micelles or quatsomes) (Battista et al., 2022b, 2019) or in which they are included (liposomes) (Battista et al., 2021, 2020b).

Our study focused on understanding the effect of mixed liposomes composition on the properties of the vesicles (entrapment efficiency, transition temperature, antiradical activity of liposomal Qu and *ex-vivo* permeability through porcine nasal mucosa). The effect of subtle differences in the molecular structure of lipids on surface properties, on the organization of the bilayer, and, as a consequence, of the physicochemical and biological behavior of the formulation was investigated in detail to point out the crucial characteristic of liposomes component for an efficient delivery of LD. Moreover, differently from what reported in literature, we included in the formulation, at the same time, a hydrophilic and a hydrophobic natural antioxidant to exploit their potential synergistic effect.

2. Materials and methods

2.1. Instrumentation

Liposomes were prepared using a Hielscher UP100-H ultrasonic processor with microtip probe (7 mm). Dynamic light scattering (DLS) and electrophoretic mobility measurements were performed using a Malvern Zetasizer Nano ZS, equipped with a 5 mW He-Ne laser operating at 633 nm. UV measurements were carried out on a DU 800 UV–vis single beam spectrophotometer (Beckman Coulter), while fluorescence measurements were carried out on a LS-50B luminescence spectrometer (Perkin Elmer). Differential scanning calorimetry (DSC) measurements were carried out using a Mettler Toledo DSC 3 calorimeter (Mettler-Toledo International Inc., Columbus, OH, USA). We performed chromatographic analysis with a Waters chromatographic system (Waters Corporation, Milford, MA, USA), consisting of a Model 600 pump, a 600 pump controller module, a 717 Plus auto-sampler, and a 996 photodiode array detector. Chromatographic data management was automated using an Empower data acquisition system (Waters S.p.A., Sesto San Giovanni MI, Italy). Eluent degassing was performed with an Agilent 1200 system (Agilent Technologies, Waldbronn, Germany). We used an analytical column (Sinergy C18. Phenomenex) with a 4 μm particle size. The eluent phase is 80% demineralized and deionized H_2O, acidified with 0.01% H_3PO_4, and 20% acetonitrile. The flow rate is 0.7 mL/min. The scanning electron microscope (ZEISS GeminiSEM 500) with an annular detector, aSTEM, was used to observe liposomes morphology.

2.2. Materials

DMPC was purchased from Avanti Polar Lipids (Alabaster, AL). Quercetin dihydrate, ascorbic acid, phosphate-buffered saline tablets (PBS, 0.0027 M KCl; 0.137 M NaCl; pH 7.4), sodium acetate, hydrogen peroxide solution (35% w/w in H_2O), 2,2′-azino-bis (3-ethylbenzothiazoline-6-sulfonic acid) diammonium salt (ABTS), dialysis tubing cellulose membrane (molecular weight cut-off = 14,000 Da) and HPLC-grade methanol, acetonitrile and chloroform were purchased from Sigma-Aldrich (Milan, Italy). LD, *N*,*N*-dimethyl-1-tetradecylamine *N*-oxide (TDAO) and *N*,*N*-dimethyl-1-tetradecylamine ammonium bromide (TDAB) surfactants were purchased from ThermoFisher Scientific (Waltham, Massachusetts), while C**14** and C**14** *N*-ox surfactants were synthesized as previously described (Battista et al., 2019). All reagents and solvents were used without further purification.

2.3. Liposomes preparation

Liposomes were prepared according to the *thin film hydration* methodology. Briefly, $1.5*10^{-5}$ moles of lipids (molar ratio between DMPC and surfactants was 9:1 or 7:3) and $3.75*10^{-7}$ moles of Qu (1:40 M ratio with respect to lipids) were dissolved in one mixture of chloroform/methanol in a round-bottom flask. The solvent was evaporated to obtain lipid films, that were stored under reduced pressure (0.4 mbar) for at least 6 h. The lipid films were hydrated with 3 mL of PBS solution containing LD (1.5 mg/mL) and AA (0.3 mg/mL), then were heated and vortex-mixed, obtaining multilamellar vesicles (MLV). Small unilamellar vesicles (SUV) were obtained after sonication in ice-water bath of the MLV solutions (8 min, 72 W, cycles 0.5 s). Total concentration of lipid was 5 mM.

Two different dialysis protocols were performed to remove unentrapped Qu and LD. For Qu, dialysis exchanging two times the external PBS solution (100 fold the liposome dispersion volume) during one hour was carried out. For LD, the liposomal solutions were previously diluted 300 fold to have a final concentration of LD equal to 5 μg/mL (to reduce the intensity of fluorescence signal) and then they were dialyzed in dark and 4 °C for three hours (100 fold the liposome dispersion volume).

2.4. Evaluation of entrapment efficiency (E.E.) of LD

The E.E. of LD was evaluated by fluorescence measurements of dispersions composed of 2.8 mL of PBS and 0.2 mL of the liposome suspension before and after dialysis (λ_{ecc} = 280 nm) and it was given by the percentage ratio between the emission value at 317 nm after and before dialysis.

2.5. Evaluation of E.E. Of Qu

The E.E. of Qu was evaluated by UV–vis measurements of solutions composed of 0.5 mL of methanol (to disrupt liposomes) and 0.5 mL of liposomes solution before and after dialysis and it was given by the percentage ratio between the absorbance value at 380 nm after and before dialysis.

2.6. DLS and ζ-potential measurements

Size, size distribution, stability and ζ-potential measurements were carried out at 25 °C on liposomes dispersions 1 mM. For stability analysis, liposomes were stored at 4 °C. Particle size analysis was performed every week for two weeks.

2.7. TEM measurements

To investigate the morphology of the aggregates 10 μL of 10 mM liposomes (loaded or not) suspensions were air-dried onto a copper grid for electron microscopy and analyzed.

2.8. Differential scanning calorimetry (DSC)

DSC measurements were performed on MLV (1 mg/10 μL, ≈ 148 mM

in total lipids) prepared according to the procedure described before, in the presence and in the absence of Qu, LD and AA. Two heating scans were recorded at a rate of 5 °C/min, followed by two heating scans recorded at a rate of 1 °C/min. Temperatures were determined with an accuracy of ± 0.1 °C and ΔH values with an accuracy of ± 0.5 kJ/mol. Three reproducible thermograms were obtained for each sample on independent samples.

2.9. Preparation of $ABTS^+$ reagent solution

Two different acetate buffer solution (pH 3.6 and pH 5.5) were prepared, followed a procedure that is described in literature (Erel, 2004). A 10 mM $ABTS^+$ solution was prepared solubilizing the ABTS diammonium salt in the acetate buffer at pH 3.6; then, a proper amount of H_2O_2 35% (w/w, final concentration 2 mM) was added and left stirring in the dark for one hour.

2.10. Evaluation of antiradical activity of free or liposomal Qu by $ABTS^+$ methodology

25 μL of $ABTS^+$ solution were rapidly added to a spectrophotometer cuvette in where were placed: 2450 μL of acetate buffer at pH 5.5 (containing NaCl for a final concentration of 150 mM), a proper amount of free Qu solution or dialyzed liposomes (depending on the E.E. of Qu of each system) and a proper amount of PBS 150 mM. The final volume was 2725 μL and the concentration of Qu in cuvette was $6.9 \bullet 10^{-7}$ M. We followed the variation of the maximal absorbance at 417 nm over one hour. All the measurements were repeated three times and then averaged.

The time constants that describe the degradation rate of $ABTS^+$ were obtained after fitting with a simple exponential decay ($y = y_0 + A_{ABTS} \bullet \exp(-x/\tau_{ABTS})$) the temporal evolution of the absorption at 417 nm. τ_{ABTS} resulted to be 28.2 min.

In the case of free and liposomal Qu, all the curves were fitted with the following equation:

$$y = y_0 + A_{Qu} \cdot \exp(-x/\tau_{Qu}) + A_{ABTS} \cdot \exp(-x/\tau_{ABTS})$$

since they showed a two processes decay. The τ_{Qu} value was obtained after fixing the parameter $\tau_{ABTS} = 28.2$ min.

2.11. Evaluation of ex-vivo permeability

Ex-vivo permeation studies were performed through porcine nasal mucosa using vertical Franz diffusion cells that were manufactured by 3D printing according to a procedure described in literature (Sil et al., 2020, 2018). Porcine snouts were obtained from a local slaughterhouse; nasal mucosa was carefully extracted and cut in pieces that were stored at −80 °C. Before using, the pieces were rinsed with PBS and then mounted in Franz cells to separate the donor compartment from the acceptor one. The effective diffusion area was 2.8 cm^2. The donor compartment was filled with 150 μL of liposomal formulation containing LD, AA and Qu while the acceptor one was filled with 2 mL of PBS. The acceptor medium was kept at 37 °C. After 3 h, 6 h and 24 h, 300 μL of each sample were withdrawn from the receiving chamber and were quickly replaced by 300 μL of PBS. Each experiment was repeated at least three times and the cumulative amount of LD permeated into the receptor compartment was determined by HPLC. The stationary phase was Sinergy C18; the mobile phase was a mixture (80/20) of 0.01% of acidified mQ water (with phosphoric acid) and acetonitrile. The flow rate was 0.7 mL/min, and the injection volume was 10 μL. Analysis were conducted at 25 °C. This method was validated for linearity (R^2 = 0.995). Each sample was diluted with methanol (1:1) and was filtered through cellulose membrane filters (0.2 μm) before injecting. The permeability percentage through the nasal mucosa was reported as the percentage ratio between the amount of LD that was found in the receiving compartment and the total amount of LD in the donating chamber.

2.12. Statistical analysis

Experiments were carried out with n = 3 in all studies. Data in all cases are expressed as means ± SD. Excel was used to evaluate the significance of differences between group means by one-way analysis of variance (oneway ANOVA) with a 95% confidence interval ($p < 0.05$ was considered to be statistically significant).

3. Results and discussion

The size and the ζ-potential of the investigated formulations, evaluated by DLS measurements, are reported in Table 1.

As expected, all the formulations containing a cationic surfactant showed positive ζ-potential even if relatively low because of the low voltage applied to avoid the risk of effects due to Joule heating: using a higher voltage with respect to the applied one we observed the blackening of the electrode surface with consequent degradation of data quality. In effect, samples containing 10 M percentage of C**14** and C**14** *N*-ox and 30 M percentage of cholesterol showed higher ζ-potentials with respect to the ones reported in this investigation, but a two-fold higher voltage was applied in that case (Battista et al., 2020b). Positive ζ-potentials were expected and observed also for aggregates containing the zwitterionic surfactants because we previously observed relatively high ζ-potential in aggregated containing C**14** *N*-ox or its analogues (Battista et al., 2022b, 2022a, 2021, 2020b). Liposomes formulated with 10 M percentage of the surfactant, loaded or not, showed the lowest ζ-potential values. Increasing the amount of the cationic component (30 M percentage) a general increase of the ζ-potential was observed. The increase is particularly relevant in the loaded formulations, which suggests electrostatic interactions of the loaded molecules with liposomes components and/or different counterion binding. Only in the case of empty DMPC/TDAB liposomes ζ-potential didn't change with 10 or 30 M percentage of the cationic component. This anomalous behavior could be ascribed to domain formation, as reported in literature in the case of mixed empty liposomes containing quaternary ammonium surfactants (Barenholz et al., 2011; Lima et al., 2013): phase segregation could bring to a peculiar lipid organization that influences the exposure of the polar headgroups to the bulk.

In general, empty liposomes showed a diameter ranging from 100

Table 1
Size (obtained from intensity weighted distributions) and ζ-potential of the investigated formulations in the presence or in the absence of LD, AA and Qu. Reported values correspond to the average values over 3 measurements. Error in ζ-potential values is within 3 mV. PdI is lower than 0.2 in all cases. [a]These samples show a statistically significant difference from their loaded counterparts.

	Empty formulations		Loaded formulation	
	Size (nm)	ζ-potential (mV)	Size (nm)	ζ-potential (mV)
DMPC	107 ± 7	−2	117 ± 7	−2
DMPC/TDAB 9:1	105 ± 9	12	92 ± 6	10
DMPC/TDAO 9:1[a]	157 ± 14	8	92 ± 9	2
DMPC/C**14** 9:1[a]	149 ± 12	12	118 ± 13	11
DMPC/C**14** *N*-ox 9:1	160 ± 13	9	140 ± 15	7
DMPC/TDAB 7:3	117 ± 9	11	121 ± 13	21
DMPC/TDAO 7:3	104 ± 7	17	90 ± 7	20
DMPC/C**14** 7:3[a]	154 ± 8	15	105 ± 11	26
DMPC/C**14** *N*-ox 7:3	114 ± 11	18	112 ± 12	22

nm to 160 nm. In some cases, the diameter of the loaded ones slightly decreases: results of the one-way ANOVA test demonstrated that the observed differences in diameter between loaded and empty liposomes are significantly different ($p < 0.05$) for three formulations (DMPC/TDAO 9:1, DMPC/C14 9:1, DMPC/C14 7:3). This evidence supports the hypothesis of the occurrence of specific electrostatic interactions between liposomes and their cargo. It is well known that the insertion of a cationic component in the bilayer influences specific characteristics (such as electric charge density, lipid packing or membrane permeability) in a concentration dependent manner. In the case of the investigated formulations the occurrence of electrostatic interactions between positively charged liposomes surface and LD and AA (ionized at the working pH) is thus not surprising. Similar consideration are reported in literature in the case of cationic liposomes loaded with LD and AA (García Esteban et al., 2018).

All the 7:3 formulations were stable for at least two weeks, while we noticed an increase of the PdI values (≈ 0.4) in 9:1 and pure DMPC formulations after 10 days. These results are probably due to the higher ζ-potential values of 7:3 formulations, which prevent aggregation.

Liposomes morphology and dimensions were also investigated by electron microscopy measurements. Some representative images of empty and loaded liposomes are shown in Fig. 1.

These images confirmed the spherical structure of vesicles and are in good agreement with DLS results. In case of DMPC formulation, the diameter of empty and loaded liposomes is about the same (≈ 100 nm, Fig. 1A and 1B), as in the case of DMPC/C14 *N*-ox 9:1 (≈ 150 nm, Fig. 1E and 1F), while empty DMPC/TDAO 9:1 liposomes show a bigger diameter than the loaded ones (Fig. 1C and 1D).

LD and the two antioxidants were added during liposomes formation by passive loading. The EE values of LD and Qu in DMPC alone and in mixed formulations, are reported in Fig. 2.

The EE of Qu was about 85%, while the EE of LD was around 15%. This difference is not surprising considering the hydrophobic and hydrophilic nature of Qu and LD, respectively. As expected, no significant differences were observed among the different formulations. We did not evaluate the EE of AA since we added it only to prevent LD oxidation.

Liposomes are characterized by a transition temperature, Tm, which is the temperature required to induce a change from an ordered gel phase, where lipids chains are tightly packed as a consequence of strong van der Waals forces, to a disordered liquid crystalline one, where phospholipids are more loosely associated. The nature of the alkyl chain (length and presence of unsaturations) mainly characterizes this phase transition. A pretransition temperature (Tp), related to the rotation of the polar headgroup of phospholipids, may be also present. DSC allows

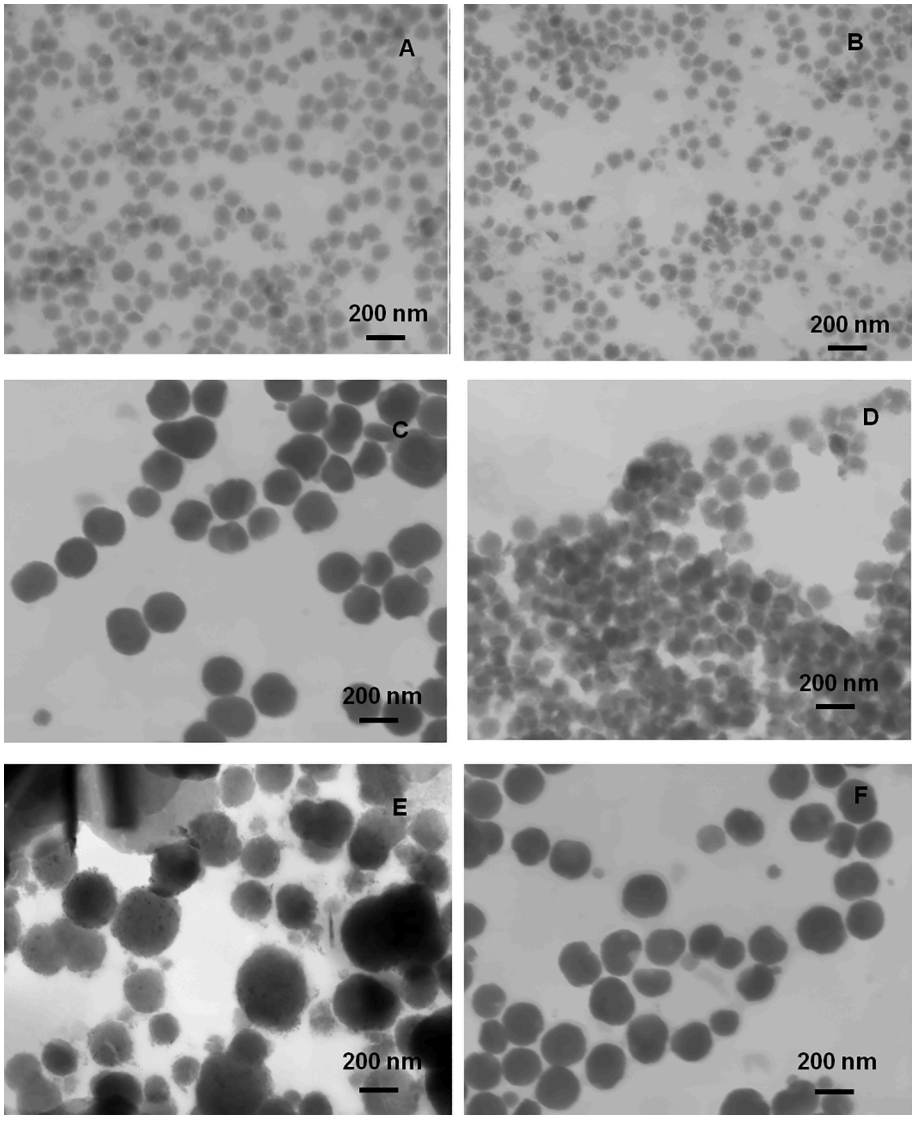

Fig. 1. TEM images of (A) empty and (B) loaded DMPC liposomes, (C) empty and (D) loaded DMPC/TDAO 9:1 liposomes and (E) empty and (F) loaded DMPC/C14 *N*-ox 9:1 liposomes.

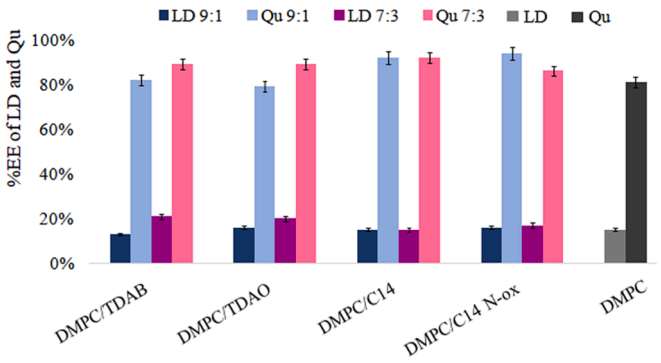

Fig. 2. EE of LD and Qu in DMPC or mixed liposomes.

the direct study of the thermal behavior of lipid bilayers: Tm and Tp can be obtained directly from the thermogram, while the corresponding enthalpy variation (ΔH) can be derived by integrating their area. In general, a high Tm value corresponds to high lipid compactness (due to strong lipid interactions); in parallel, this is reflected in high ΔH values. The inclusion of a surfactant and/or hydrophobic molecules in a pure lipid bilayer may lead to a variation of the shape of the peaks, Tm and/or ΔH values, giving useful information regarding lipids interaction, their miscibility, the presence of domains and the influence of the solutes included in the lipid bilayer. In this work, we used MLV in order to prevent complex thermograms given by the fusion into larger aggregates during the scans, which are commonly observed for unilamellar vesicles (Drazenovic et al., 2015).

The thermograms and the relative thermodynamic parameters of the investigated loaded and not loaded MLV are reported in Fig. 3 and Table 2 - 3.

The thermograms relative to loaded or empty DMPC/surfactant 9:1 liposomes showed, in most cases, an increase of Tm values indicating a higher compactness of the bilayer with respect to pure DMPC. As mentioned before, the interaction among the alkyl chains contributes to the main transition to a greater extent if compared to the nature of the polar headgroup. Evidently, despite the structural differences between DMPC and the minor component, the same length of their chains minimizes the possible disturbing effect of the micelle forming surfactant. In good agreement, ΔH values remain almost unaltered in mixed bilayers with respect to DMPC one, with the exception of DMPC/C**14** and DMPC/C**14** *N*-ox not loaded liposomes.

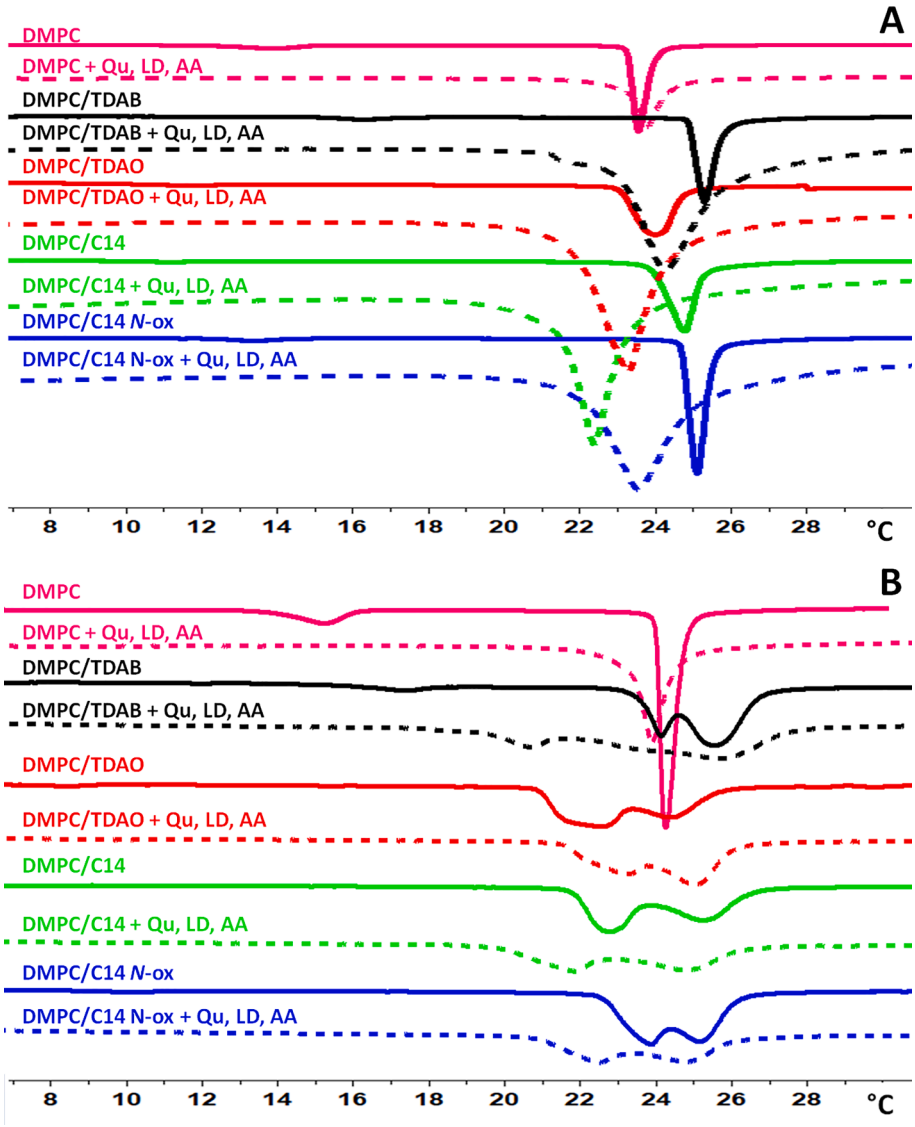

Fig. 3. Comparison between empty (full lines) and containing Qu, LD and AA formulations (dashed lines) of DMPC and (A): DMPC/surfactant 9:1 liposomes or (B) DMPC/surfactant 7:3 liposomes. Scan rate is 1° C/min.

Table 2
Thermodynamic parameters obtained by DSC measurements on empty and loaded with Qu, LD and AA, DMPC/surfactant 9:1 liposome formulations. Empty and loaded DMPC liposomes are also reported for comparison. Uncertainties are ± 0.1 °C for the temperature values and ± 0.5 J/g for the ΔH values.

Formulation (9:1)	Tp (°C)	Tm (°C)	ΔH (J/g)
DMPC	14.0	24.1	27.9
DMPC + Qu, LD, AA	/	23.8	27.5
DMPC/TDAB	16.3	25.3	27.6
DMPC/TDAB + Qu, LD, AA	/	25.1	28.4
DMPC/TDAO	12.8	24.0	30.8
DMPC/TDAO + Qu, LD, AA	/	24.5	29.2
DMPC/C**14**	11.7	24.8	33.2
DMPC/C**14** + Qu, LD, AA	/	24.0	24.2
DMPC/C**14** *N*-ox	13.4	25.1	39.7
DMPC/C**14** *N*-ox + Qu, LD, AA	/	24.7	27.8

Table 3
Thermodynamic parameters obtained by DSC measurements on empty and loaded with Qu, LD and AA, DMPC/surfactant 7:3 liposome formulations. Empty and loaded DMPC liposomes are also reported for comparison. Uncertainties are ± 0.1 °C for the temperature values and ± 0.5 J/g for the ΔH values.

Formulation (7:3)	Tp (°C)	Tm (°C)	ΔH (J/g)
DMPC	14.0	24.1	27.9
DMPC + Qu, LD, AA	/	23.8	27.5
DMPC/TDAB	17.2	24.0, 25.5	31.0
DMPC/TDAB + Qu, LD, AA	/	20.6, 25.5	33.4
DMPC/TDAO	/	22.0, 24.4	30.0
DMPC/TDAO + Qu, LD, AA	/	22.9, 25.0	29.3
DMPC/C**14**	/	22.7, 25.5	29.7
DMPC/C**14** + Qu, LD, AA	/	21.8, 24.8	27.3
DMPC/C**14** *N*-ox	/	23.6, 25.2	31.8
DMPC/C**14** *N*-ox + Qu, LD, AA	/	22.3, 24.8	23.2

In the presence of the solutes the pretransition disappears in all 9:1 formulations indicating that they are nearby or located in a region of the bilayer close to the headgroups, in agreement with literature results for Qu (Drăguşin et al., 2010; Liu and Guo, 2006). In fact, although Qu is a very hydrophobic molecule scarcely soluble in water (Abraham and Acree, 2014) and it would be expected to find it deeply in the bilayer, it seems that its hydroxyl groups can interact with the polar headgroups of lipids. It is known that Qu has five exchangeable protons with pK_a values from 6 to 13 units, and it exists in three different anionic forms at physiological pH (Álvarez-Diduk et al., 2013). Probably, the microenvironment surrounding the headgroup of liposomes favors the partial deprotonation of the hydroxyl groups of Qu and, consequently, the electrostatic attraction between the negatively charged antioxidant and the polar groups of lipids.

When the percentage of the synthetic surfactant increases from 10% to 30% the thermograms showed the disappearance of the pretransition with exception of TDAB containing liposomes (**SI 1**): this indication, together with the fact that DMPC/TDAB liposomes 9:1 feature the highest Tp (at least 3 °C of difference with the other formulations), suggests that particularly strong interactions establish in the headgroup region that remain unaltered even increasing the amount of the cationic component. A broadening and a splitting of the main peak appeared in the thermograms either in the presence and in the absence of Qu. This evidence indicates the presence of a phase separation in liposomes bilayer probably due to the poor miscibility of the components at this molar percentage. Literature reports confirm that phase separation also occurs in void mixed liposomes containing quaternary ammonium surfactants bearing or not the *L*-prolinol moiety (Barenholz et al., 2011; Lima et al., 2013). In particular, in the case of empty DMPC/TDAB 7:3 liposomes the predominant peak appears at 25.5 °C, the same temperature at which the peak relative to the main transition occurs in the thermogram of 9:1 liposomes: this evidence, together with the presence of Tp, suggests that lipid organization in most part of the bilayer is very similar in liposomes containing 10 or 30 M percentage of TDAB. The broadening of the peak at lower temperature is more evident in Qu loaded liposomes with respect to not loaded ones (with the exception of DMPC/TDAO) indicating that the antioxidant preferentially accumulates in the corresponding domain. The ΔH values are quite similar and decrease only when Qu is included in DMPC/C**14** and DMPC/C**14** *N*-ox liposomes, as observed in 9:1 formulations. As a whole, liposomes containing the synthetic surfactants bearing the pyrrolidinium ring showed a similar thermotropic behavior whereas liposomes containing the acyclic analogues exhibited peculiar thermotropic properties probably due to the different organization in the headgroup region and exposure of the charged groups, as confirmed by the trend in ζ-potential values.

Antiradical activity of free and loaded Qu was evaluated through the $ABTS^{+}$ methodology: this molecule in its oxidized state has a green colour that disappears when it is reduced, giving a colorless solution. The rate of this process is related to the concentration and antiradical capacity of the system. The degradation of $ABTS^{+}$ was monitored spectrophotometrically over time in the absence or in the presence of free and liposomal Qu (Fig. 4).

As expected, when $ABTS^{+}$ reacted with free Qu (cyano dashed line) its degradation was sensitively much faster compared to when it was alone (grey dashed line). Indeed, Qu is one of the most efficient antioxidants among flavonoids due to its two antioxidant pharmacophores and its ability to scavenge free radicals and bind transition metal ions (Ozgen et al., 2016). When Qu is included in liposomal formulations of DMPC or containing the 10% of acyclic surfactants, its antiradical activity increases, especially with TDAB. This result can be explained considering that Qu in the latter formulation gives rise to a specific interaction with the polar headgroups region (as indicated by Tp values) affecting its ability to scavenge $ABTS^{+}$. In general, the antioxidant activity of a molecule is strictly influenced by the polarity of its microenvironment (Oehlke et al., 2010; Shang et al., 2010) and, for aqueous solutions, by the pH of the medium (Galano et al., 2011; León-Carmona et al., 2012). Based on ζ-potential values, Qu in DMPC/TDAB liposomes experiences a more polar environment with respect to the almost neutral DMPC and DMPC/TDAO liposomes. On the other hand, after an initial burst the formulation containing C**14** *N*-ox surfactant showed a slowdown of the antiradical activity of Qu after twenty minutes (blue line in Fig. 4**A**), while the formulation containing the C**14** surfactant (green line in Fig. 4**A**) shows a behavior comparable to free Qu. Despite the fact that the ζ-potential values of these formulations are similar to the TDAB one, lipid organization is different as suggested by DSC results. This can imply a different hydration of the polar headgroups and/or a different water penetration near them with a consequent effect on the antiradical activity of Qu due to its different accessibility and microenvironment polarity. The folding of the pyrrolidinium ring of *N*-ox (Battista et al., 2020b) could explain the reason why this formulation behaves differently from the others. In agreement with this behavior, we observed that the antiradical activity of a natural compound, (+)-usnic acid, included in micelles composed of pure C**14** or C**14** *N*-ox strongly depends on the nature of the polar headgroups. Differently from Qu, the antiradical activity of (+)-usnic acid significantly increased when it was embedded in liposomes containing 10 M percentage of C**14** *N*-ox (Battista et al., 2019). This evidence confirms that the antiradical activity of a molecule embedded in the bilayer does not depend only on its intrinsic properties but is primarily affected by its interaction with lipids and even subtle modifications of their molecular structure can be relevant.

When the molar fraction of surfactant raised up to 30%, Qu antiradical activity increases in all the mixed formulations investigated with respect to corresponding 9:1 formulations, in particular for the cationic ones (see **Figure SI2** for a direct comparison). Probably the presence of Qu rich domain, as suggested by DSC results, increases the Qu local concentration, and reasonably affects (in a manner depending on domain properties) its interaction with the radical cation. The only exception was TDAO containing liposomes probably because in these

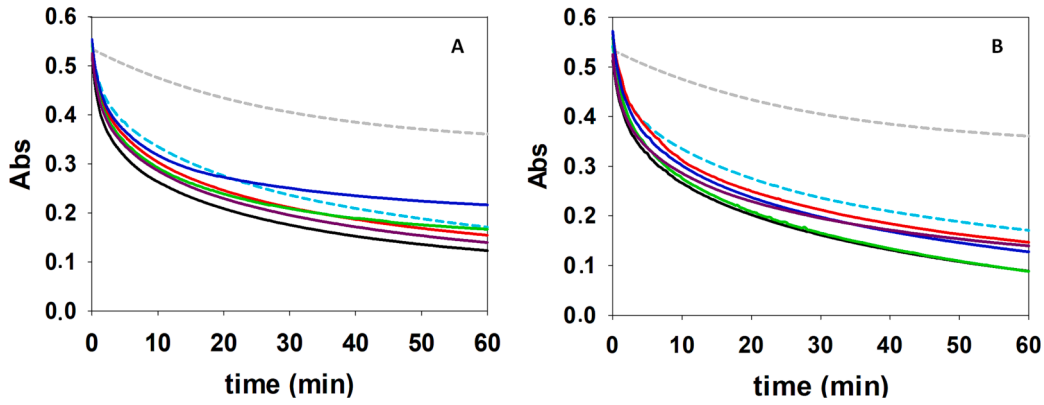

Fig. 4. Kinetic measurements of $ABTS^{+}$ degradation in the absence or in the presence of free and loaded Qu for 9:1 formulations (**A**) and 7:3 formulations (**B**): free $ABTS^{+}$ (grey dashed line), free Qu (cyano dashed line), DMPC/TDAB (dark line), DMPC/TDAO (red line), DMPC/C**14** (green line), DMPC/C**14** *N*-ox (blue line), DMPC (purple line). (For interpretation of the references to colour in this figure legend, the reader is referred to the web version of this article.)

aggregates Qu seems not to segregate in preferential domain.

Each curve was fitted with an exponential decay by two processes (as reported in the experimental section) with the exception of the curve related to the spontaneous degradation of free $ABTS^{+}$ that was fitted with a simple exponential decay. The obtained time constant τ indicates the time necessary for the half of the $ABTS^{+}$ present in solution to be reduced due to the interaction with Qu, thus give an information on the rapidity of the reaction between $ABTS^{+}$ and Qu free or loaded in the investigated systems. The τ estimated by the data analysis are reported in Fig. 5.

It is observable that in most cases either with free or liposomal Qu similar results were obtained. This evidence indicates that liposomal Qu preserves its antioxidant activity. This can be considered a good result taking into account that part of the liposomal Qu is not accessible to $ABTS^{+}$ since it is embedded in a deeper region of the bilayer (and thus can't be reached by a radical cation). Obviously, differences in the compactness of the bilayer can affect the possibility of $ABTS^{+}$ to reach Qu in the bilayer.

The capacity of free and liposomal LD to cross the nasal mucosa was evaluated by *ex-vivo* permeability studies using vertical Franz diffusion cells. First of all, we verified that lipids did not interact with our 3D printed cells performing the Stewart assay on the liposomal solution that came into contact with them for 24 h (data not shown). For the permeability tests we did not separate unloaded LD from liposomes because its amount in solution is too high (and thus the procedure too long) to be removed with dialysis without LD degradation. Porcine nasal mucosa was used since it is the most similar to the human one (Wadell et al., 1999) and the experiments were performed at 37 °C, corresponding to the temperature of human nose. PBS buffer (150 mM, pH 7.4) was used as receptor medium (Gavini et al., 2010) in order to mimic physiologic conditions.

HPLC analyses were conducted for this evaluation because porcine mucosa released substances in the acceptor compartment which interfered with the fluorescence of levodopa.

The percentage of LD in the presence of loaded liposomes that crossed the mucosa after 3 and 6 h was lower than 1%, so in Fig. 6 we reported only the percentage after 24 h. Surprisingly, the amount of free LD that crosses the nasal mucosa was very high (above 90%), probably because of its very small dimensions and its relatively low water solubility with respect to the aggregates.

The fact that a lower amount of LD with respect to free LD reaches the acceptor compartment in the presence of loaded liposomes indicates that the aggregates tend to remain inside the membrane and plug it at an extent depending on the formulation: with neutral DMPC liposomes we

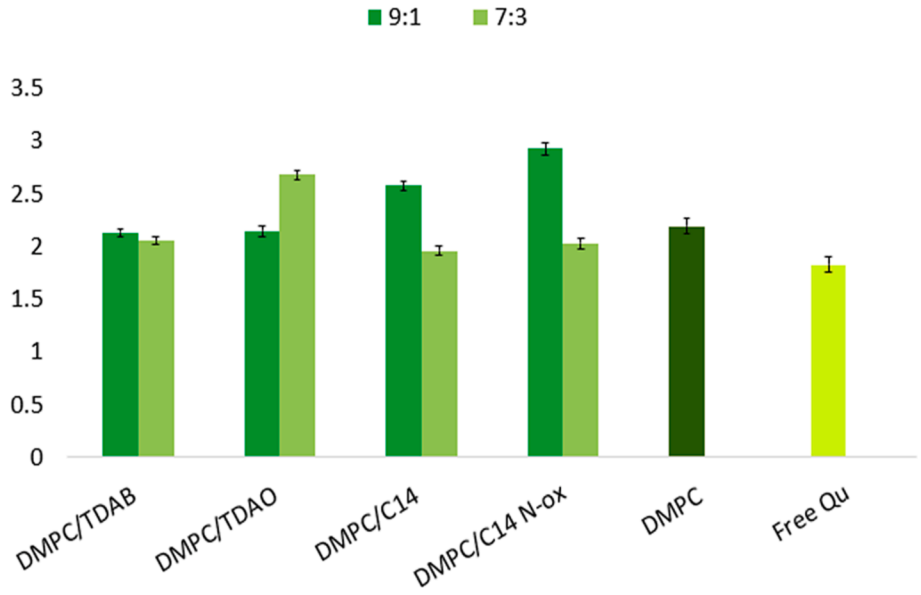

Fig. 5. Comparison of τ_{Qu} relative to of $ABTS^{+}$ degradation curve in the presence of free or liposomal Qu for 9:1 and 7:3 formulations. The reported errors correspond to the standard error obtained from the fit.

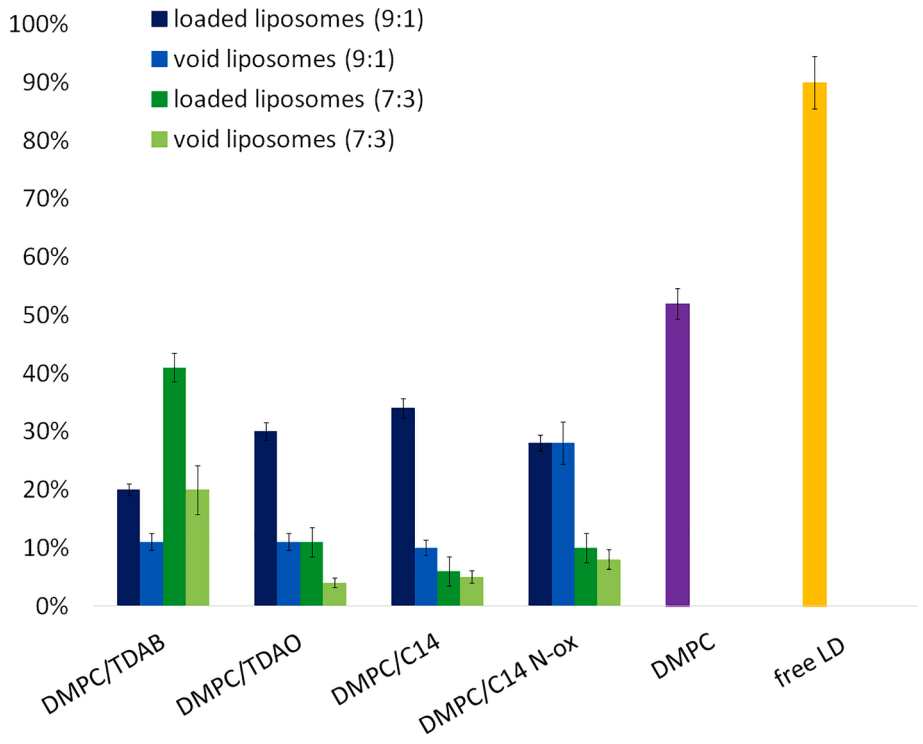

Fig. 6. Comparison of the percentage of LD that crosses the porcine nasal mucosa after 24 h, for the different liposome formulations and for free LD.

found the highest percentage of LD in the acceptor compartment while in the case of formulations containing the 30% of TDAO, C**14** and C**14** *N*-ox no more than 10% of LD reached it. This result suggests that the strength of the interaction of the aggregates with negatively charged nasal mucosa is proportional to their ζ-potential values (see Table 1). In fact, the same mixed formulations containing the 10% of surfactant show lower ζ-potential values and higher LD permeability compared to the analogue formulations with the 30% of surfactant. The only exception was the formulation containing the 30% of TDAB, which features a potential similar to the other 7:3 formulations. This evidence indicates that liposomes potential is not the only parameter that controls their interaction with biological membranes but also polar head group exposure, structure (cationic or *N*-ox) and counterion association play a crucial role. To quantify the effect of liposomes on the reduction of LD nasal membrane permeability, we carried out the same experiments in which empty liposomes and free drug were added together in the donor compartment of Franz cells. In all cases, the amount of LD that passes the mucosa is lower in the presence of empty liposomes than with loaded ones (Fig. 6). This result indicates that, even if some liposomes remain trapped in the membrane, the amount that is allowed to pass achieves the vehiculation of the drug.

4. Conclusions

The purpose of this work was to investigate the structure–activity relationship of different levodopa-loaded liposomes and to undertake preliminary analysis of their potential application as intranasal drug delivery system. DLS, TEM and DSC analysis confirmed the formation of mixed liposomes and the incorporation of surfactants into the lipid bilayer. As a whole, our results point out that ζ-potential is not the only parameter that influences the interaction with biological negative membranes, but also lipid organization and the compactness of the bilayer play a crucial role, as observed for Qu antiradical activity. The cationic formulation DMPC/TDAB 7:3 is the most promising for LD intranasal delivery: the EE of LD, the Qu antiradical activity and the *ex-vivo* permeability through nasal mucosa were the highest ones between the mixed formulations. Despite the evidence that the percentage of LD that reaches the acceptor compartment is lower for the liposome loaded LD than for the free one, the results are still interesting and promising because: *i*) the presence of a drug delivery system protects LD from oxidation, *ii*) it is known that free LD shows side effects (Hauser, 2009) and *iii*) only a small amount of the free drug can reach the brain if administered intravenously.

CRediT authorship contribution statement

Elena Allegritti: Conceptualization, Investigation, Data curation, Writing – original draft. **Sara Battista:** Resources, Data curation, Formal analysis, Writing – original draft. **Maria Anna Maggi:** Methodology, Data curation, Investigation. **Claudia Marconi:** Investigation, Data curation. **Luciano Galantini:** Supervision, Writing – review & editing. **Luisa Giansanti:** Conceptualization, Supervision, Project administration, Writing – review & editing.

Declaration of Competing Interest

The authors declare that they have no known competing financial interests or personal relationships that could have appeared to influence the work reported in this paper.

Data availability

Data will be made available on request.

Acknowledgments

We kindly thank Mr. Giuseppe Del Giudice for providing us porcine snouts, Dr. Pierangelo Bellio (University of L'Aquila) for the preparation of the nasal mucosa and Dr. Lorenzo Arrizza (Center of Microscopy of the University of L'Aquila) for his support with TEM images acquisition.

Appendix A. Supplementary data

Supplementary data to this article can be found online at https://doi.org/10.1016/j.ijpharm.2023.123230.

References

Abbina, S., Parambath, A., 2018. PEGylation and its alternatives: A summary. Eng. Biomater. Drug Deliv. Syst. Beyond Polyethyl. Glycol 363–376. https://doi.org/10.1016/B978-0-08-101750-0.00014-3.

Abraham, M.H., Acree, W.E., 2014. On the solubility of quercetin. J. Mol. Liq. 197, 157–159. https://doi.org/10.1016/j.molliq.2014.05.006.

Abri Aghdam, M., Bagheri, R., Mosafer, J., Baradaran, B., Hashemzaei, M., Baghbanzadeh, A., de la Guardia, M., Mokhtarzadeh, A., 2019. Recent advances on thermosensitive and pH-sensitive liposomes employed in controlled release. J. Control. Release 315, 1–22. https://doi.org/10.1016/j.jconrel.2019.09.018.

Al Asmari, A.K., Ullah, Z., Tariq, M., Fatani, A., 2016. Preparation, characterization, and in vivo evaluation of intranasally administered liposomal formulation of donepezil. Drug Des. Devel. Ther. 10, 205–215. https://doi.org/10.2147/DDDT.S93937.

Álvarez-Diduk, R., Ramírez-Silva, M.T., Galano, A., Merkoçi, A., 2013. Deprotonation mechanism and acidity constants in aqueous solution of flavonols: A combined experimental and theoretical study. J. Phys. Chem. B 117, 12347–12359. https://doi.org/10.1021/jp4049617.

Barenholz, Y., Bombelli, C., Bonicelli, M.G., di Profio, P., Giansanti, L., Mancini, G., Pascale, F., 2011. Influence of lipid composition on the thermotropic behavior and size distribution of mixed cationic liposomes. J. Colloid Interface Sci. 356, 46–53. https://doi.org/10.1016/j.jcis.2010.11.062.

Battista, S., Campitelli, P., Carlone, A., Giansanti, L., 2019. Influence of structurally related micelle forming surfactants on the antioxidant activity of natural substances. Chem. Phys. Lipids 225, 104818. https://doi.org/10.1016/J.CHEMPHYSLIP.2019.104818.

Battista, S., Bellio, P., Celenza, G., Galantini, L., Franceschini, I., Mancini, G., Giansanti, L., 2020a. Correlation of Physicochemical and Antimicrobial Properties of Liposomes Loaded with (+)-Usnic Acid. Chempluschem 85, 1014–1021. https://doi.org/10.1002/cplu.202000125.

Battista, S., Campitelli, P., Galantini, L., Köber, M., Vargas-Nadal, G., Ventosa, N., Giansanti, L., 2020b. Use of N-oxide and cationic surfactants to enhance antioxidant properties of (+)-usnic acid loaded liposomes. Colloids Surfaces A Physicochem. Eng. Asp. 585, 124154 https://doi.org/10.1016/J.COLSURFA.2019.124154.

Battista, S., Maggi, M.A., Bellio, P., Galantini, L., D'Archivio, A.A., Celenza, G., Colaiezzi, R., Giansanti, L., 2020c. Curcuminoids-loaded liposomes: influence of lipid composition on their physicochemical properties and efficacy as delivery systems. Colloids Surfaces A Physicochem. Eng. Asp. 597 https://doi.org/10.1016/j.colsurfa.2020.124759.

Battista, S., Köber, M., Vargas-Nadal, G., Veciana, J., Giansanti, L., Ventosa, N., 2021. Homogeneous and stable (+)-usnic acid loaded liposomes prepared by compressed CO2. Colloids Surfaces A Physicochem. Eng. Asp. 624, 126749 https://doi.org/10.1016/J.COLSURFA.2021.126749.

Battista, S., Bellio, P., Fagnani, L., Allegritti, E., Nazzicone, L., Galantini, L., Celenza, G., Giansanti, L., 2022a. Structurally Related Liposomes Containing N-Oxide Surfactants: Physicochemical Properties and Evaluation of Antimicrobial Activity in Combination with Therapeutically Available Antibiotics. Mol. Pharm. 19, 788–797. https://doi.org/10.1021/acs.molpharmaceut.1c00609.

Battista, S., Mariana, K., Bellio, P., Celenza, G., Galantini, L., Vargas-nadal, G., Fagnani, L., Veciana, J., Ventosa, N., Giansanti, L., 2022b. Quatsomes Formulated with. https://doi.org/10.1021/acsanm.1c04365.

Bnyan, R., Khan, I., Ehtezazi, T., Saleem, I., Gordon, S., O'Neill, F., Roberts, M., 2018. Surfactant Effects on Lipid-Based Vesicles Properties. J. Pharm. Sci. 107, 1237–1246. https://doi.org/10.1016/j.xphs.2018.01.005.

Bombelli, C., Bordi, F., Ferro, S., Giansanti, L., Jori, G., Mancini, G., Mazzuca, C., Monti, D., Ricchelli, F., Sennato, S., Venanzi, M., 2008. New cationic liposomes as vehicles of m-tetrahydroxyphenylchlorin in photodynamic therapy of infectious diseases. Mol. Pharm. 5, 672–679. https://doi.org/10.1021/mp800037d.

Bombelli, C., Stringaro, A., Borocci, S., Bozzuto, G., Colone, M., Giansanti, L., Sgambato, R., Toccaceli, L., Mancini, G., Molinari, A., 2010. Efficiency of liposomes in the delivery of a photosensitizer controlled by the stereochemistry of a gemini surfactant component. Mol. Pharm. 7, 130–137. https://doi.org/10.1021/mp900173v.

Bordi, F., Cerichelli, G., De Berardinis, N., Diociaiuti, M., Giansanti, L., Mancini, G., Sennato, S., 2010. Synthesis and physicochemical characterization of new twin-tailed N-oxide based gemini surfactants. Langmuir 26, 6177–6183. https://doi.org/10.1021/la1005067.

Brandl, M., 2001. Liposomes as drug carriers: A technological approach. Biotechnol. Annu. Rev. 7, 59–85. https://doi.org/10.1016/S1387-2656(01)07033-8.

Costantino, H.R., Illum, L., Brandt, G., Johnson, P.H., Quay, S.C., 2007. Intranasal delivery: Physicochemical and therapeutic aspects. Int. J. Pharm. 337, 1–24. https://doi.org/10.1016/J.IJPHARM.2007.03.025.

Darden, L., 2007. Mechanisms and models. Cambridge Companion to Philos. Biol. 39, 139–159. https://doi.org/10.1017/CCOL9780521851282.008.

Drăguşin, M., Ţugulea, L., Ganea, C., 2010. The effects of the natural antioxidant quercetin and anions of the Hofmeister series on liposomes marked with chlorophyll a. Gen. Physiol. Biophys. 29, 41–49. https://doi.org/10.4149/gpb_2010_01_41.

Drazenovic, J., Wang, H., Roth, K., Zhang, J., Ahmed, S., Chen, Y., Bothun, G., Wunder, S.L., 2015. Effect of lamellarity and size on calorimetric phase transitions in single component phosphatidylcholine vesicles. Biochim. Biophys. Acta - Biomembr. 1848, 532–543. https://doi.org/10.1016/j.bbamem.2014.10.003.

Emad, N.A., Ahmed, B., Alhalmi, A., Alzobaidi, N., Al-Kubati, S.S., 2021. Recent progress in nanocarriers for direct nose to brain drug delivery. J. Drug Deliv. Sci. Technol. 64, 102642 https://doi.org/10.1016/j.jddst.2021.102642.

Erel, O., 2004. A novel automated direct measurement method for total antioxidant capacity using a new generation, more stable ABTS radical cation. Clin. Biochem. 37, 277–285. https://doi.org/10.1016/J.CLINBIOCHEM.2003.11.015.

Feitosa, E., Adati, R.D., Karlsson, G., 2023. The role of counterion and concentration on the thermal behavior and structure of dioctadecyldimethylammonium bromide and chloride in water. Thermochim. Acta 724. https://doi.org/10.1016/j.tca.2023.179498.

Ferreira, J.J., Rocha, J.F., Falcão, A., Santos, A., Pinto, R., Nunes, T., Soares-da-Silva, P., 2015. Effect of opicapone on levodopa pharmacokinetics, catechol-O-methyltransferase activity and motor fluctuations in patients with Parkinson's disease. Eur. J. Neurol. 22, 815–e56. https://doi.org/10.1111/ene.12666.

Filograna, R., Beltramini, M., Bubacco, L., Bisaglia, M., 2016. Anti-Oxidants in Parkinson's Disease Therapy: A Critical Point of View. Curr. Neuropharmacol. 14, 260–271. https://doi.org/10.2174/1570159x13666151030102718.

Fitzpatrick, B., 1950. of Melanin Formation. Physiol. Rev. 30, 91–126.

Gabizon, A., Papahadjopoulos, D., 1992. The role of surface charge and hydrophilic groups on liposome clearance in vivo. BBA - Biomembr. 1103, 94–100. https://doi.org/10.1016/0005-2736(92)90061-P.

Galano, A., Alvarez-Idaboy, J.R., Francisco-Márquez, M., 2011. Physicochemical insights on the free radical scavenging activity of sesamol: Importance of the acid/base equilibrium. J. Phys. Chem. B 115, 13101–13109. https://doi.org/10.1021/jp208315k.

García Esteban, E., Cózar-Bernal, M.J., Rabasco Álvarez, A.M., González-Rodríguez, M.L., 2018. A comparative study of stabilising effect and antioxidant activity of different antioxidants on levodopa-loaded liposomes. J. Microencapsul. 35, 357–371. https://doi.org/10.1080/02652048.2018.1487473.

Gavini, E., Rassu, G., Sanna, V., Cossu, M., Giunchedi, P., 2010. Mucoadhesive microspheres for nasal administration of an antiemetic drug, metoclopramide: in-vitro/ex-vivo studies. J. Pharm. Pharmacol. 57, 287–294. https://doi.org/10.1211/0022357055623.

Giansanti, L., Mauceri, A., Galantini, L., Altieri, B., Piozzi, A., Mancini, G., 2016. Glucosylated pH-sensitive liposomes as potential drug delivery systems. Chem. Phys. Lipids 200, 113–119. https://doi.org/10.1016/j.chemphyslip.2016.08.004.

Guo, X., Zheng, H., Guo, Y., Wang, Y., Anderson, G.J., Ci, Y., Yu, P., Geng, L., Chang, Y. Z., 2017. Nasal delivery of nanoliposome-encapsulated ferric ammonium citrate can increase the iron content of rat brain. J. Nanobiotechnology 15, 1–13. https://doi.org/10.1186/s12951-017-0277-2.

Gurturk, Z., Tezcaner, A., Dalgic, A.D., Korkmaz, S., Keskin, D., 2017. Maltodextrin modified liposomes for drug delivery through the blood-brain barrier. Medchemcomm 8, 1337–1345. https://doi.org/10.1039/c7md00045f.

Hauser, R.A., 2009. Levodopa: Past, present, and future. Eur. Neurol. 62, 1–8. https://doi.org/10.1159/000215875.

Hong, S.S., Oh, K.T., Choi, H.G., Lim, S.J., 2019. Liposomal formulations for nose-to-brain delivery: Recent advances and future perspectives. Pharmaceutics 11, 1–18. https://doi.org/10.3390/pharmaceutics11100540.

Ishigami, T., Suga, K., Umakoshi, H., 2015. Chiral Recognition of l -Amino Acids on Liposomes Prepared with l -Phospholipid. ACS Appl. Mater. Interfaces 7, 21065–21072. https://doi.org/10.1021/acsami.5b07198.

Jenner, P., 2003. Oxidative Stress in Parkinson's Disease. Ann Neurol 53, 26–38. https://doi.org/10.1002/ana.10483.

Jin, H., Kanthasamy, A., Ghosh, A., Anantharam, V., Kalyanaraman, B., Kanthasamy, A. G., 2014. Mitochondria-targeted antioxidants for treatment of Parkinson's disease: Preclinical and clinical outcomes. Biochim. Biophys. Acta - Mol. Basis Dis. 1842, 1282–1294. https://doi.org/10.1016/j.bbadis.2013.09.007.

Karanth, H., Murthy, R.S.R., 2010. pH-Sensitive liposomes-principle and application in cancer therapy. J. Pharm. Pharmacol. 59, 469–483. https://doi.org/10.1211/jpp.59.4.0001.

Karukstis, K.K., McDonough, J.R., 2005. Characterization of the aggregates of N-Alkyl-N-methylpyrrolidinium bromide surfactants in aqueous solution. Langmuir 21, 5716–5721. https://doi.org/10.1021/la047015l.

Kleszczyńska, H., Sarapuk, J., Oświęcimska, M., Witek, S., 2000. Antioxidative activity of some quaternary ammonium salts incorporated into erythrocyte membranes. Zeitschrift fur Naturforsch. - Sect. C J. Biosci. 55, 976–980. https://doi.org/10.1515/znc-2000-11-1221.

Krasowska, A., Piasecki, A., Murzyn, A., Sigler, K., 2007. Assaying the antioxidant and radical scavenging properties of aliphatic mono- and Di-N-oxides in superoxide dismutase-deficient yeast and in a chemiluminescence test. Folia Microbiol. (Praha) 52, 45–51. https://doi.org/10.1007/BF02932137.

León-Carmona, J.R., Alvarez-Idaboy, J.R., Galano, A., 2012. On the peroxyl scavenging activity of hydroxycinnamic acid derivatives: Mechanisms, kinetics, and importance of the acid-base equilibrium. Phys. Chem. Chem. Phys. 14, 12534–12543. https://doi.org/10.1039/c2cp40651a.

Lewińska, A., Kulbacka, J., Domżał-Kędzia, M., Witwicki, M., 2021. Antiradical properties of n-oxide surfactants—two in one. Int. J. Mol. Sci. 22 https://doi.org/10.3390/ijms22158040.

Lewitt, P.A., 2008. Levodopa for the Treatment of Parkinson ' s Disease. N. Engl. J. Med. 359, 2468–2476.

Lima, L.M.C., Giannotti, M.I., Redondo-Morata, L., Vale, M.L.C., Marques, E.F., Sanz, F., 2013. Morphological and nanomechanical behavior of supported lipid bilayers on addition of cationic surfactants. Langmuir 29, 9352–9361. https://doi.org/10.1021/la400067n.

Liskayová, G., Hubčík, L., Búcsi, A., Fazekaš, T., Martínez, J.C., Devínsky, F., Pisárčik, M., Hanulová, M., Ritz, S., Uhríková, D., 2019. PH-Sensitive N, N-Dimethylalkane-1-amine N-Oxides in DNA Delivery: From Structure to Transfection Efficiency. Langmuir 35, 13382–13395. https://doi.org/10.1021/acs.langmuir.9b02353.

Liu, W., Guo, R., 2006. Interaction between flavonoid, quercetin and surfactant aggregates with different charges. J. Colloid Interface Sci. 302, 625–632. https://doi.org/10.1016/J.JCIS.2006.06.045.

Marwah, M., Perrie, Y., Badhan, R.K.S., Lowry, D., 2020. Intracellular uptake of EGCG-loaded deformable controlled release liposomes for skin cancer. J. Liposome Res. 30, 136–149. https://doi.org/10.1080/08982104.2019.1604746.

Mohamed, M., Abu Lila, A.S., Shimizu, T., Alaaeldin, E., Hussein, A., Sarhan, H.A., Szebeni, J., Ishida, T., 2019. PEGylated liposomes: immunological responses. Sci. Technol. Adv. Mater. 20, 710–724. https://doi.org/10.1080/14686996.2019.1627174.

Oehlke, K., Heins, A., Stöckmann, H., Schwarz, K., 2010. Impact of emulsifier microenvironments on acid-base equilibrium and activity of antioxidants. Food Chem. 118, 48–55. https://doi.org/10.1016/j.foodchem.2009.04.078.

Oliveira, A.C.N., Sárria, M.P., Moreira, P., Fernandes, J., Castro, L., Lopes, I., Côrte-Real, M., Cavaco-Paulo, A., Real Oliveira, M.E.C.D., Gomes, A.C., 2016. Counter ions and constituents combination affect DODAX:MO nanocarriers toxicity: In vitro and in vivo. Toxicol. Res. (Camb) 5, 1244–1255. https://doi.org/10.1039/c6tx00074f.

Ozgen, S., Kilinc, O.K., Selamoglu, Z., 2016. Antioxidant Activity of Quercetin: A Mechanistic Review Kuersetinin Antioksidan Aktivitesi: Mekanik Bir Derleme. Turkish J. Agric. -Food Sci. Technol. 4, 1134–1138.

Piasecki, A., Piłakowska-Pietras, D., Baran, A., Krasowska, A., 2008. Synthesis and properties of surface chemically pure alkylamidoamine-N- oxides at the air/water interface. J. Surfactants Deterg. 11, 187–194. https://doi.org/10.1007/s11743-008-1070-x.

Resende, J., Azevedo, D., Chevalier, Y., Carit, A.C., Arquier, D., Buri, M. V, Riske, K.A., Ricci, G., Bolzinger, A., 2023. Elastic cationic liposomes for vitamin C delivery : Development , characterization and skin absorption study 638. 10.1016/j.ijpharm.2023.122897.

Riaz, M.K., Riaz, M.A., Zhang, X., Lin, C., Wong, K.H., Chen, X., Zhang, G., Lu, A., Yang, Z., 2018. Surface functionalization and targeting strategies of liposomes in solid tumor therapy: A review. Int. J. Mol. Sci. 19 https://doi.org/10.3390/ijms19010195.

Shang, Y.J., Jin, X.L., Shang, X.L., Tang, J.J., Liu, G.Y., Dai, F., Qian, Y.P., Fan, G.J., Liu, Q., Zhou, B., 2010. Antioxidant capacity of curcumin-directed analogues: Structure-activity relationship and influence of microenvironment. Food Chem. 119, 1435–1442. https://doi.org/10.1016/j.foodchem.2009.09.024.

Shang, X., Liu, Y., Yan, E., Eisenthal, K.B., 2001. Effects of counterions on molecular transport across liposome bilayer: Probed by second harmonic generation. J. Phys. Chem. B 105, 12816–12822. https://doi.org/10.1021/jp0120918.

Sil, B.C., Alvarez, M.P., Zhang, Y., Kung, C.P., Hossain, M., Iliopoulos, F., Luo, L., Crowther, J.M., Moore, D.J., Hadgraft, J., Lane, M.E., Hilton, S.T., 2018. 3D-printed Franz type diffusion cells. Int. J. Cosmet. Sci. 40, 604–609. https://doi.org/10.1111/ics.12504.

Sil, B.C., Belgrave, R.G., Alvarez, M.P., Luo, L., Cristofoli, M., Penny, M.R., Moore, D.J., Hadgraft, J., Hilton, S.T., Lane, M.E., 2020. 3D-Printed Franz cells – update on optimization of manufacture and evaluation. Int. J. Cosmet. Sci. 42, 415–419. https://doi.org/10.1111/ics.12618.

Singh, S.K., Bajpai, M., Tyagi, V.K., 2006. Amine Oxides: A Review. J. Oleo Sci. 55, 99–119. https://doi.org/10.5650/jos.55.99.

Tai, K., He, X., Yuan, X., Meng, K., Gao, Y., Yuan, F., 2017. A comparison of physicochemical and functional properties of icaritin-loaded liposomes based on different surfactants. Colloids Surfaces A Physicochem. Eng. Asp. 518, 218–231. https://doi.org/10.1016/j.colsurfa.2017.01.019.

Varshosaz, J., Taymouri, S., Pardakhty, A., Asadi-shekaari, M., Babaee, A., 2014. 816103.Pdf 2014.

Wadell, C., Björk, E., Camber, O., 1999. Nasal drug delivery - Evaluation of an in vitro model using porcine nasal mucosa. Eur. J. Pharm. Sci. 7, 197–206. https://doi.org/10.1016/S0928-0987(98)00023-2.

Wang, C., Wang, X., Wang, D., Qian, S., Zhang, F., Li, M., Li, M., Lu, W., Liu, B., Qing, G., 2023. Remarkable difference of phospholipid molecular chirality in regulating PrP aggregation and cell responses. Chinese Chem. Lett. 34, 107332 https://doi.org/10.1016/j.cclet.2022.03.055.

Xiang, Y., Wu, Q., Liang, L., Wang, X., Wang, J., Zhang, X., Pu, X., Zhang, Q., 2012. Chlorotoxin-modified stealth liposomes encapsulating levodopa for the targeting delivery against the Parkinson's disease in the MPTP-induced mice model. J. Drug Target. 20, 67–75. https://doi.org/10.3109/1061186X.2011.595490.

Zheng, X., Shao, X., Zhang, C., Tan, Y., Liu, Q., Wan, X., Zhang, Q., Xu, S., Jiang, X., 2015. Intranasal H102 Peptide-Loaded Liposomes for Brain Delivery to Treat Alzheimer's Disease. Pharm. Res. 32, 3837–3849. https://doi.org/10.1007/s11095-015-1744-9.